Shortest-path fractal dimension for percolation in two and three dimensions

Zongzheng Zhou, Ji Yang, Youjin Deng, and Robert M. Ziff

Shortest-Path Fractal Dimension for Percolation in Two and Three Dimensions

Zongzheng Zhou[1], Ji Yang[1], Youjin Deng[1*], Robert M. Ziff[2†]

[1]*Hefei National Laboratory for Physical Sciences at the Microscale and Department of Modern Physics,*
University of Science and Technology of China, Hefei, Anhui 230027, PR China and
[2]*Michigan Center for Theoretical Physics and Department of Chemical Engineering,*
University of Michigan, Ann Arbor, Michigan 48109-2136, USA

We carry out a high-precision Monte Carlo study of the shortest-path fractal dimension $d_{\min}$ for percolation in two and three dimensions, using the Leath-Alexandrowicz method which grows a cluster from an active seed site. A variety of quantities are sampled as a function of the chemical distance, including the number of activated sites, a measure of the radius, and the survival probability. By finite-size scaling, we determine $d_{\min} = 1.130\,77(2)$ and $1.375\,6(6)$ in two and three dimensions, respectively. The result in 2D rules out the recently conjectured value $d_{\min} = 217/192$ [Phys. Rev. E **82**, 020102(R) (2010)].

As a standard model of disordered system [1, 2], percolation has been intensively studied over the last 50 years and applied to many other fields due to its richness in both mathematic and physics. The nature of phase transition of percolation has been well established. In particular, within the two-dimensional (2D) university class, there are only few critical exponents left to be expressed exactly, among which is the shortest-path fractal dimension $d_{\min}$, defined by [2–4]

$$\langle \ell \rangle \sim r^{d_{\min}}, \tag{1}$$

where r is the Euclidean distance between two sites belonging to the same cluster, and ℓ is the shortest path.

The shortest path ℓ between two sites in a cluster is the minimum number of steps on a path of occupied bonds/sites in the cluster, and was first studied independently by several groups in the early 1980's [5–9]. The length ℓ is also called the chemical distance [10]. A related quantity is the spreading dimension d_ℓ [11], which describes the scaling of the mass $\mathcal{N}$ of a critical cluster within a chemical distance ℓ as $\mathcal{N} \sim \ell^{d_\ell}$, and is related to the fractal dimension d_f of the cluster by $d_\ell = d_f/d_{\min}$.

In percolation, the shortest-path naturally occurs during epidemic growth or burning algorithms. Previous measurements of $d_{\min}$ in 2D include $d_{\min} = 1.18(4)$ [6], $1.118(15)$ [7], $1.15(3)$ [10], $1.102(13)$ [12], $1.132(4)$ [13], $1.130(2)$ [14], $1.130\,7(4)$ [3], $1.130\,6(3)$ [15] and $1.1303(8)$ [16]. A summary of the early work is given in Ref. [13].

In 1984, Havlin and Nossal [10] conjectured $d_{\min} = d_f - 1/\nu = 91/48 - 3/4 = 55/48 = 1.145833$, which was soon shown to be too large [13, 14]. In 1987 Larsson speculated that $d_{\min}$ could be $17/16$ or even 1, but these are both excluded. In 1988 Herrmann and Stanley conjectured $d_{\min} = 2 - d_B + d_{\rm red}$, where $d_{\rm red} = 1/\nu = 3/4$ is the "red"-bond dimension and d_B is the backbone

dimension. Using Deng, Blöte and Neinhuis's result $d_B = 1.6434(2)$ [17] (see also [18, 19]), we find this prediction gives $d_{\min} = 2 - 1.6434(2) + 0.75 = 1.1066(2)$, which is too small. In 1989, Tzschichholz, Bunde and Havlin [20] considered $d_{\min} = 53/48 = 1.1041666...$, which is also below measured values. In 1992, Grassberger conjectured $d_{\min} = 26/23 = 1.130434783...$ based upon numerical results, and consistent with existing measurements.

In 1998, Porto et al. conjectured that $d_{\min}$ is related to a pair-connectivity scaling exponent g_1 by $d_{\min} = g_1 + \beta/\nu$ where $\beta = 5/36$ for 2D. However, g_1 was later shown to have the exact value $g_1 = 25/24$ [15, 21], which implies $d_{\min} = 55/48 = 1.145833$, identical to Havlin and Nossal's earlier conjecture [10].

In 2010, one of us (Deng) and his coauthors conjectured an exact expression [16] of $d_{\min}$ for the 2D critical and tricritical random-cluster model: $d_{\min} = (g + 2)/(g + 18)/32g$, where g is the Coulomb-gas coupling constant, related to the random cluster fugacity q by relation $g = (2/\pi)\cos^{-1}(q/2 - 1)$. This conjecture is numerically correct up to the third or fourth decimal place for all values of q studied in Ref. [16]. For the $q \to 1$ limit—i.e., standard bond percolation—the predicted value $d_{\min} = 217/192 = 1.130208$ was consistent with the numerical results in previous works [6, 7, 10, 12–15]. In addition, the conjectured formula exhibits other good properties. It reproduces the exact results for the critical uniform spanning tree ($q \to 0$) as well as for the tricritical $q \to 0$ Potts model; at the tricritical $q \to 0$ point, the derivative with respect to q is also correct.

The main goal of the present work is to carry out a high-precision Monte Carlo test of the conjecture in Ref. [16] in the context of 2D percolation. A numerical estimate of $d_{\min}$ for 3D percolation is also provided. Some preliminary results of this work were reported in a recent paper on biased directed percolation [22].

We simulate bond percolation on the square and the simple-cubic lattice by the Leath-Alexandrowicz algorithm [6, 23], which grows a percolation cluster starting from a seed site. For each neighboring edge of the seed

---
[*]Email: yjdeng@ustc.edu.cn
[†]Email: rziff@umich.edu

site an occupied bond is placed with occupation probability p, and the neighboring site is activated and added into the growing cluster. After all the neighboring edges of the seed site have been visited, the growing procedure is continued from the newly added sites. This proceeds until no more new sites can be added into the cluster (the procedure dies out) or the initially set maximum time step $\ell_{\max}$ is reached.

The above procedure is also called breadth-first growth, and ℓ is equal to the shortest-path length between the seed site and any activated sites at time step ℓ. We set $\ell = 1$ for the beginning of the growth, and measure the number of activated sites $N(\ell)$ as a function of ℓ. In addition, we record the Euclidean distance r_i of each activated site i to the seed site, and define a radius by

$$R(\ell) = \begin{cases} 0 & \text{if } N(\ell) = 0 \\ \sqrt{\sum_{i=1}^{N} r_i^2} & \text{if } N(\ell) \geq 1 \ . \end{cases} \quad (2)$$

The statistical averages, $\mathcal{N}(\ell) \equiv \langle N(\ell) \rangle$ and $\mathcal{R}(\ell) \equiv \langle R(\ell) \rangle$, and the associated error bars are calculated. We also sample the survival probability $\mathcal{P}(\ell)$ that at time step ℓ, the growing procedure still survives.

At criticality, one expects scaling behavior

$$\mathcal{N}(\ell) \sim \ell^{Y_N}\ , \quad \mathcal{R}(\ell) \sim \ell^{Y_R}\ , \quad \mathcal{P}(\ell) \sim \ell^{-Y_P}\ , \quad (3)$$

where critical exponents Y_P, Y_N, and Y_R are related to β, ν and $d_{\min}$ by

$$\begin{aligned} Y_N &= \frac{\gamma}{\nu d_{\min}} - 1, \quad Y_P = \frac{\beta}{\nu d_{\min}}, \\ Y_R &= \frac{\gamma + 2\nu}{\nu d_{\min}} - 1\ , \end{aligned} \quad (4)$$

with $\gamma = d\nu - 2\beta$ and d equal to the spatial dimensionality. In terms of exponents of epidemic processes [24], these quantities correspond to $\delta = Y_P$, $\eta = Y_N$, and $1/z - \delta = Y_R$.

To eliminate the unknown non-universal constants in front of the scaling behaviors (3), we define ratio $Q_\mathcal{O}(\ell) = \mathcal{O}(2\ell)/\mathcal{O}(\ell)$ for $\mathcal{O} = \mathcal{N}, \mathcal{R}$ and $\mathcal{P}$. In the $\ell \to \infty$ limit, one has

$$Y_N = \log_2(Q_\mathcal{N}),\ Y_R = \log_2(Q_\mathcal{R}),\ Y_P = -\log_2(Q_\mathcal{P}). \quad (5)$$

In 2D, one has the exactly known exponents $\beta = 5/36$, $\nu = 4/3$, and $\gamma = 43/18$ [1, 25–28]. In 3D, the exact values are unknown, and are numerically found to be $\beta/\nu = 0.4774(1)$ and $\nu = 0.8764(7)$ [29–33].

Initial estimate of $d_{\min}$ for 2D. We first carried out simulations at the critical point $p = 1/2$ for bond percolation on the square lattice with time step up to $\ell_{\max} = 1024$ and the number of samples about 2×10^9.

The asymptotic behavior of the observables $\mathcal{N}$, $\mathcal{R}$ and $\mathcal{P}$ is expected to follow the form

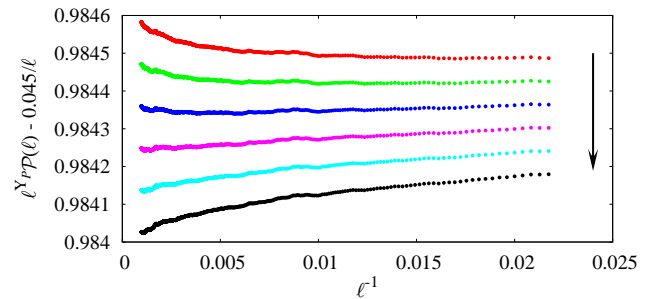$$\mathcal{O}(\ell) = \ell^Y (a_0 + b_1 \ell^{y_1} + b_2 \ell^{-2})\ , \quad (6)$$

FIG. 1: (Color online) Plot of $\mathcal{P}\ell^{Y_P} - 0.045\ell^{-1}$ versus ℓ^{-1} in 2D. The Y_P value is obtained via Eq. (4) by setting $d_{\min}$ at 1.1302, 1.1304, 1.1306, 1.1308, 1.1310 and 1.1312, following the arrow.

where higher-order corrections are neglected and the critical exponent Y is given by Eq. (3). The leading finite-size correction exponent is known to be $y_1 = -0.96(6) \approx -1$ [22]. A least-squares criterion was used to fit the data assuming the above form. With y_1 being fixed at -1, the fit of $\mathcal{P}$ gives $d_{\min} = 1.1308 \pm 0.0002$ and $b_1 = 0.045(5)$, and the fit of $\mathcal{N}$ yields $d_{\min} = 1.1308 \pm 0.0002$.

As an illustration, we plot $\mathcal{P}\,\ell^{Y_P} - 0.045\ell^{-1}$ in Fig. 1 and $\mathcal{N}\ell^{-Y_N}$ in Fig. 2, both vs. ℓ^{-1}, where the $d_{\min}$ value is set at a series of values in range $[1.1302, 1.1312]$ in steps of 0.0002, including the above estimate $d_{\min} = 1.1308$. The term $-0.045\ell^{-1}$ is included in Fig. 1 to remove the overall slope seen in the data of $\mathcal{P}$; we did not do this to the $\mathcal{N}$ data (Fig. 2), and there the slope is evident. The values of Y_P and Y_N are obtained from Eq. (4), using the exactly known values of β and ν. Because the leading corrections have been subtracted in Fig. 1, it is expected that the curve for the correct $d_{\min}$ value should asymptotically become flat and reach a constant. Figure 1 shows that as ℓ increases, the curve for the conjectured value $217/192 \approx 1.1302$ is bending up while the curve for 1.1312 is bending down. This implies that the correct $d_{\min}$ value should fall somewhere in between. A similar behavior is seen in Fig. 2, where the curve for 1.1308 is approximately straight while those for 1.1302 and 1.1312 are bending down and up, respectively.

Further simulations for 2D. Although the conjectured number $217/192$ seems to be ruled out by the data shown in Figs. 1 and 2, a more careful analysis is still desirable. The above analysis makes an assumption that the leading correction is governed by ℓ^{-1}, but the physical origin of this term is unclear as the leading irrelevant thermal scaling field has exponent $y_i = -2$. It is conceivable that more slowly convergent corrections exist but are not detected by the simulations up to $\ell_{\max}=1024$. In particular, percolation can be regarded as a special case of biased-directed percolation with the symmetry between spatial and temporal directions restored [22]. In this case, multiplicative and/or additive logarithmic corrections can occur in principle such that the scaling behavior of $\mathcal{N}, \mathcal{R}$
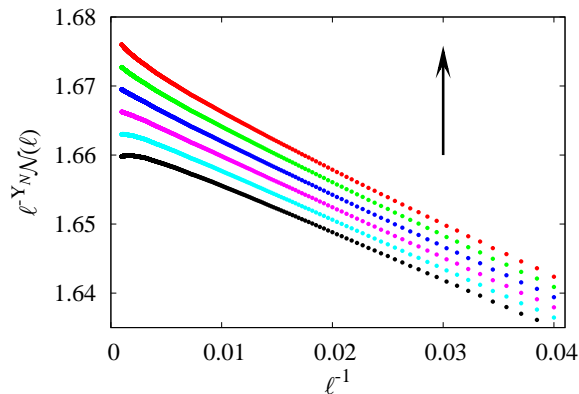
FIG. 2: (Color online) Plot of $\mathcal{N}\ell^{-Y_N}$ versus ℓ^{-1} in 2D. The Y_N value is obtained via Eq. (4) by setting $d_{\min}$ at 1.1302, 1.1304, 1.1306, 1.1308, 1.1310 and 1.1312, following the arrow.

and $\mathcal{P}$ is modified as

$$\mathcal{O}(\ell) \sim [\log(\ell/\ell_0)]^{y_m} \ell^Y \; (1 + 1/[\log(\ell/\ell_1)]^{y_c}) \; , \qquad (7)$$

where ℓ_0 and ℓ_1 are constants, and y_m and y_c are the associated correction exponents. Corrections of the $\log\log\ell$ form are also possible. We note that due to cancellation between nominator and denominator, the multiplicative logarithmic correction will not explicitly appear in ratio $Q_{\mathcal{O}}$ ($\mathcal{O}=\mathcal{N}$, $\mathcal{R}$, $\mathcal{P}$), for which the scaling behavior is modified as

$$Q_{\mathcal{O}}(\ell) = 2^Y \left(1 + 1/[\log(\ell/\ell_1)]^{y_c'}\right) \; , \qquad (8)$$

where y_c' can be equal to y_c or $|y_m|$, depending on the relative amplitudes of the terms associated with them.

To investigate this, we carried out more extensive simulations up to $\ell_{\max} = 16384$. The number of samples was 4.5×10^{10} for $\ell \le 1024$, 5×10^9 for $1024 < \ell \le 4096$, 10^9 for $4096 < \ell \le 8192$, and 3×10^8 for $\ell > 8192$.

From the $Q_{\mathcal{O}}$ data, we calculate the $d_{\min}(\ell)$ value by Eqs. (4) and (5). Table I displays the resulting values of $d_{\min}(\ell)$ from the ratios $Q_{\mathcal{N}}$, $Q_{\mathcal{R}}$ and $Q_{\mathcal{P}}$. It can be clearly seen that for $\ell \le 3072$, the $d_{\min}$ values that derive from $\mathcal{N}$ and $\mathcal{R}$ increase monotonically as ℓ increases. Further, by looking at the $d_{\min}^{(\mathcal{N})}(L)$ or the $d_{\min}^{(\mathcal{R})}(L)$ data for $L = 1024, 2048, 4096$ and 8192, one can safely conclude that the asymptotic value $d_{\min}$ is *larger* than 1.1307. For clarity, these data are plotted in Fig. 3. The conjecture $d_{\min} = 217/192$ would mean that the monotonically increasing curves for $d_{\min}^{(\mathcal{N})}$ and $d_{\min}^{(\mathcal{R})}$ must bend downward as ℓ become larger, and thus a very rapid drop would occur near origin ($1/\ell \to 0$) in the inset of Fig. 3, which seems very unlikely. The $d_{\min}^{(\mathcal{P})}$ data are less accurate and not shown in Fig. 3.

We fit the $d_{\min}(\ell)$ data by

$$d_{\min}(\ell) = d_{\min} + b_1 \, \ell^{y_1} + b_2 \, \ell^{-2} \; , \qquad (9)$$

ℓ	$d_{\min}^{(\mathcal{N})}$	$d_{\min}^{(\mathcal{R})}$	$d_{\min}^{(\mathcal{P})}$
12	1.112 909(3)	1.102 251(2)	1.099 42(3)
16	1.117 007(4)	1.109 204(2)	1.106 44(3)
24	1.121 303(4)	1.116 112(2)	1.114 18(3)
32	1.123 540(4)	1.119 588(2)	1.118 10(3)
48	1.125 835(4)	1.123 109(2)	1.122 14(3)
64	1.127 007(4)	1.124 902(2)	1.124 20(3)
96	1.128 215(4)	1.126 743(2)	1.126 32(3)
128	1.128 826(4)	1.127 685(2)	1.127 38(3)
192	1.129 445(4)	1.128 647(2)	1.128 44(3)
256	1.129 755(4)	1.129 140(2)	1.128 99(3)
384	1.130 083(4)	1.129 653(2)	1.129 57(3)
512	1.130 251(4)	1.129 914(2)	1.129 83(3)
768	1.130 42(2)	1.130 180(6)	1.130 15(9)
1024	1.130 49(2)	1.130 317(6)	1.130 36(9)
1536	1.130 58(2)	1.130 455(7)	1.130 33(9)
2048	1.130 63(2)	1.130 532(7)	1.130 27(9)
3072	1.130 70(3)	1.130 61(2)	1.130 5(2)
4096	1.130 68(3)	1.130 62(2)	1.130 6(2)
6144	1.130 72(7)	1.130 65(4)	1.130 9(5)
8192	1.130 80(7)	1.130 72(4)	1.130 8(5)

TABLE I: Results for $d_{\min}$ from $Q_{\mathcal{N}}$, $Q_{\mathcal{R}}$ and $Q_{\mathcal{P}}$ in 2D.
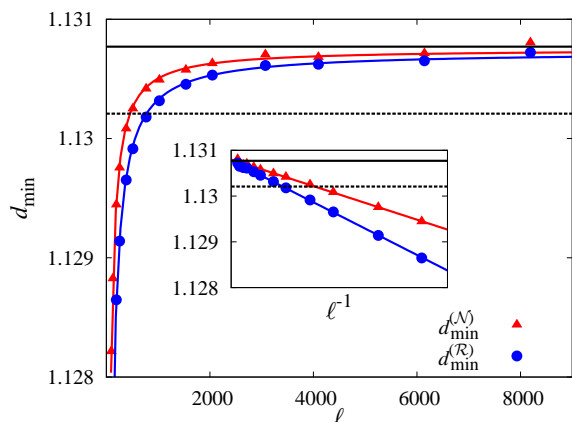

FIG. 3: (Color online) Plot of $d_{\min}$ versus ℓ in 2D, deduced from $Q_{\mathcal{N}}$ and $Q_{\mathcal{R}}$. The inset shows $d_{\min}$ versus ℓ^{-1}. The solid and dashed horizontal lines correspond to $d_{\min} = 1.13077$ and $217/192$, respectively. The red (upper) and blue (lower) curves are obtained from the fits.

using a least-squares criterion. The data for small $\ell < \ell_{\min}$ were gradually excluded to see how the residual χ^2 changes with respect to $\ell_{\min}$. Table II lists the fitting results for $d_{\min}^{(\mathcal{N})}$, $d_{\min}^{(\mathcal{R})}$ and $d_{\min}^{(\mathcal{P})}$. From these fits, we obtain $d_{\min}^{(\mathcal{N})} = 1.130\,77(3)$, $d_{\min}^{(\mathcal{R})} = 1.130\,77(2)$ and $d_{\min}^{(\mathcal{P})} = 1.130\,66(15)$. Note that to account for potential systematic errors, the error bars in these final estimates are taken to be significantly larger than those statistical ones in Tab. II. Considering the stability of the fit results in Tab. II, we believe that the estimated error margins are reliable. We note that the coefficient b_2 cannot be determined well in the fits for $\ell_{\min} > 32$. Thus, fits with $b_2 = 0$ were also carried out, and the results agree with

	$\ell_{\min}$	χ^2	d.o.f	$d_{\min}$	b_1	b_2	y_1
$d_{\min}^{(\mathcal{N})}$	16	13	15	1.130 759(5)	−0.206(2)	0.15(2)	−0.961(3)
	24	12	14	1.130 764(6)	−0.202(4)	0.12(3)	−0.957(5)
	32	12	13	1.130 763(8)	−0.204(6)	0.13(6)	−0.958(7)
	48	11	12	1.130 766(10)	−0.20(1)	0.1(2)	−0.95(1)
	64	7	11	1.130 780(12)	−0.18(2)	0.4(3)	−0.93(2)
$d_{\min}^{(\mathcal{R})}$	24	20	14	1.130 776(4)	−0.265(2)	−0.19(2)	−0.918(2)
	32	13	13	1.130 771(4)	−0.270(3)	−0.14(3)	−0.922(2)
	48	12	12	1.130 768(5)	−0.273(5)	−0.08(7)	−0.925(4)
	64	10	11	1.130 772(7)	−0.266(7)	−0.2(2)	−0.920(5)
$d_{\min}^{(\mathcal{P})}$	16	8	15	1.130 67(4)	−0.39(2)	0.41(9)	−0.99(1)
	24	8	14	1.130 66(5)	−0.40(4)	0.5(3)	−0.99(2)
	32	8	13	1.130 66(6)	−0.41(5)	0.6(5)	−0.99(3)
	48	8	11	1.130 65(7)	−0.4(1)	0.8(11)	−1.00(5)
	64	8	11	1.130 64(8)	−0.4(2)	1(2)	−1.01(8)

TABLE II: Fitting results of $d_{\min}$ in 2D, for various cutoffs $\ell_{\min}$. "d.o.f." stands for "degrees of freedom."

FIG. 4: (Color online) Plot of $d_{\min}^{(\mathcal{N})}$ and $d_{\min}^{(\mathcal{R})}$ versus $\ell^{-0.7}$ in 3D.

ℓ	$d_{\min}^{(\mathcal{N})}$	$d_{\min}^{(\mathcal{R})}$	$d_{\min}^{(\mathcal{P})}$
12	1.364 7(2)	1.358 44(8)	1.357 6(4)
16	1.365 4(2)	1.363 14(8)	1.359 7(4)
24	1.366 8(2)	1.367 22(8)	1.363 1(4)
32	1.367 9(2)	1.369 01(9)	1.365 6(4)
48	1.369 4(2)	1.370 69(9)	1.368 4(4)
64	1.370 4(2)	1.371 52(9)	1.369 9(4)
96	1.371 6(2)	1.372 42(9)	1.371 8(4)
128	1.372 3(2)	1.372 94(9)	1.372 8(4)
192	1.373 1(2)	1.373 50(9)	1.373 8(4)
256	1.373 5(2)	1.373 78(9)	1.374 4(4)
384	1.374 1(2)	1.374 19(9)	1.375 0(4)
512	1.374 4(2)	1.374 49(9)	1.375 3(4)
768	1.374 6(2)	1.374 7(2)	1.375 4(5)
1024	1.374 6(3)	1.374 7(2)	1.376 0(5)

TABLE III: Results for $d_{\min}$ from $Q_{\mathcal{N}}$, $Q_{\mathcal{R}}$ and $Q_{\mathcal{P}}$ in 3D.

	$\ell_{\min}$	χ^2	d.o.f	$d_{\min}$	b_1	b_2	y_1
$d_{\min}^{(\mathcal{N})}$	8	6	11	1.376 1(3)	−0.062(7)	0.50(5)	−0.57(4)
	12	3	10	1.375 7(3)	−0.08(2)	0.7(2)	−0.64(6)
	16	2	9	1.375 6(4)	−0.09(3)	0.9(3)	−0.68(8)
	24	2	8	1.375 4(4)	−0.12(6)	1.4(9)	−0.7(2)
	32	2	7	1.375 3(4)	−0.2(1)	2(2)	−0.8(2)
$d_{\min}^{(\mathcal{R})}$	8	7	11	1.375 4(2)	−0.045(4)	−1.99(3)	−0.60(3)
	12	2	10	1.375 7(3)	−0.035(5)	−1.13(7)	−0.53(5)
	16	2	9	1.375 8(3)	−0.033(6)	−1.2(2)	−0.51(6)
	24	2	8	1.375 7(4)	−0.03(1)	−1.1(3)	−0.52(9)
	32	2	7	1.375 7(4)	−0.04(2)	−0.9(6)	−0.6(2)
$d_{\min}^{(\mathcal{P})}$	8	7	11	1.376 6(4)	−0.19(4)	1.0(2)	−0.80(6)
	12	4	10	1.376 5(5)	−0.23(8)	1.3(5)	−0.8(1)
	16	3	9	1.376 5(5)	−0.2(1)	1.3(9)	−0.8(2)
	24	3	8	1.376 5(7)	−0.2(2)	1(2)	−0.8(3)

TABLE IV: Fitting results of $d_{\min}$ in 3D.

our above estimates of $d_{\min}$.

We also simulated critical site percolation on an $L \times L$ triangular lattice with periodic boundary conditions; this system is known to have zero amplitude of the leading irrelevant scaling field with exponent $y_i = -2$. A row of lattice sites was chosen, and all the occupied sites on this row were assumed to belong to the same cluster. The Leath-Alexandrowicz method was then used to grow the cluster. The chemical radius ℓ of the completed cluster was measured. From scaling $\ell \sim L^{d_{\min}}$, we determine $d_{\min} = 1.130\,7(1)$, also ruling out the conjectured value.

Results for 3D. We simulated bond percolation on the simple-cubic lattice at the central value of the recently estimated critical point $p = 0.248\,811\,8(1)$ [33], which is slightly below the previous value of $p = 0.248\,812\,6(5)$ [34]. The simulation was carried up to $\ell_{\max} = 2048$, with the number of samples 7×10^9 for $\ell \le 1024$ and 2×10^9 for $\ell > 1024$. Analogous to the procedure on the square lattice, we sampled $\mathcal{N}$, $\mathcal{R}$, $\mathcal{P}$ and studied the ratios $Q_{\mathcal{N}}$, $Q_{\mathcal{R}}$, $Q_{\mathcal{P}}$. The values of $d_{\min}^{(\mathcal{O})}$ deduced from these ratios
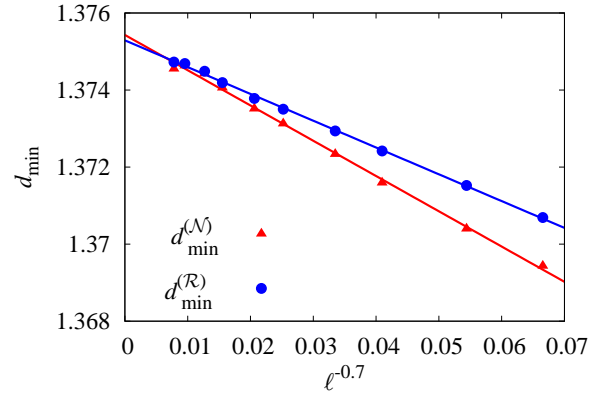
with $\beta/\nu = 0.4774(1)$ are listed in Table III. The fitting results are shown in Table IV and yield $d_{\min}^{(\mathcal{N})} = 1.375\,6(6)$, $d_{\min}^{(\mathcal{R})} = 1.375\,7(6)$, $d_{\min}^{(\mathcal{P})} = 1.376\,5(10)$, and $y_1 = -0.7(2)$. The data of $d_{\min}^{(\mathcal{N})}(\ell)$ and $d_{\min}^{(\mathcal{R})}(\ell)$ versus $\ell^{-0.7}$ are further shown in Fig. 4, where the exponent 0.7 reflects the value of y_1.

In conclusion, we determined the shortest-path fractal dimension $d_{\min}$ for percolation in 2D and 3D to be $1.130\,77(2)$ and $1.375\,6(6)$ respectively. For the 2D value, we use the result which follows from $\mathcal{R}(\ell)$ and has the smallest error bars. To our knowledge, these are the most accurate values currently available. The conjectured value in 2D, $d_{\min} = 217/192$ [16], is ruled out with a high probability. Grassberger's earlier conjecture $d_{\min} = 26/23$ [3] is also ruled out. The 3D result represents a substantial increase in precision over the previous values of 1.34(1) [14] and 1.374(4) [4].

[1] D. Stauffer and A. Aharony, *Introduction to Percolation Theory*, 2nd ed. (Taylor and Francis, London, 1994).
[2] A. Bunde and S. Havlin, in *Fractals and Disordered Systems*, 2nd ed., edited by A. Bunde and S. Havlin (Springer, New York, 1996).
[3] P. Grassberger, J. Phys. A **25**, 5475 (1992).
[4] P. Grassberger, J. Phys. A **25**, 5867 (1992).
[5] P. Grassberger, Math. Biosciences **63**, 157 (1983).
[6] Z. Alexandrowicz, Phys. Lett. A **80**, 284 (1980).
[7] R. Pike and H. E. Stanley, J. Phys. A **14**, L169 (1981).
[8] H. J. Herrmann, D. C. Hong and H. E. Stanley, J. Phys. A **17**, L261 (1984).
[9] K. M. Middlemiss, S. G. Whittington, and D. S. Gaunt, J. Phys. A **13**, 1835 (1980).
[10] S. Havlin and R. Nossal, J. Phys. A **17**, L427 (1984).
[11] J. Vannimenus, J. P. Nadal, and H. Martin, J. Phys. A **17**, L351 (1984).
[12] R. Rammal, J. C. Angles d'Auriac, and A. Benoit, J. Phys. A **17**, L491 (1984).
[13] P. Grassberger, J. Phys. A **18**, L215 (1985).
[14] H. J. Herrmann and H. E. Stanley, J. Phys. A **21**, L829 (1988).
[15] P. Grassberger, J. Phys. A **32**, 6233 (1999).
[16] Y. Deng, W. Zhang, T. M. Garoni, A. D. Sokal, and A. Sportiello, Phys. Rev. E **81**, 020102(R) (2010).
[17] Y. Deng, H. W. J. Blöte, B. Nienhuis, Phys. Rev. E **69**, 026114 (2004).
[18] P. Grassberger, Physica A **262**, 251 (1999).
[19] J. L. Jacobsen and P. Zinn-Justin, Phys. Rev E **66**, 055102 (R) (2002).
[20] F. Tzschichholz, A. Bunde, and S. Havlin, Phys. Rev. A **39**, 5470 (1989).
[21] R. M. Ziff, J. Phys. A **32**, L457 (1999).
[22] Z. Zhou, J. Yang, R. M. Ziff and Y. Deng, arXiv:1109.6567.
[23] P. L. Leath, Phys. Rev. B **14**, 5046 (1976).
[24] P. Grassberger and A. de la Torre, Annals Phys. (N.Y.) **122**, 373 (1979).
[25] J. L. Cardy, Nucl. Phys. B **240**, 514 (1984).
[26] S. Smirnov, W. Werner, Math. Research Lett. **8**, 729 (2001).
[27] G. F. Lawler, O. Schramm, W. Werner, Electron. J. Probab. **7**, 2 (2002).
[28] H. Kesten, Comm. Math. Phys. **109**, 109 (1987).
[29] Y. Deng and H. W. J. Blöte, Phys. Rev. E **72**, 016126 (2005).
[30] P. H. L. Martins and J. A. Plascak, Phys. Rev. E **67**, 046119 (2003).
[31] Y. Tomita and Y. Okabe, J. Phys. Soc. Jpn. **71**, 1570 (2002).
[32] H. G. Ballesteros, L. A. Fernández, V. Martín-Mayor, A. Muñoz Sudupe, G. Parisi, and J. J. Ruiz-Lorenzo, J. Phys. A **32**, 1 (1999).
[33] J. Wang, Z. Zhou, Q. Liu, Y. Deng, in preparation.
[34] C. D. Lorenz and R. M. Ziff, Phys. Rev. E **57**, 230 (1998).